

High-Spin Radical Cations of Poly(*m*–*p*-anilines) and Poly(*m*–*p*–*p*-anilines): Synthesis and Spectroscopic Properties

Marta Gałecka,[†] Ireneusz Wielgus,[†] Małgorzata Zagórska,[†] Mariusz Pawłowski,[‡] and Irena Kulszewicz-Bajer^{*,†}

Faculty of Chemistry, Warsaw University of Technology, Noakowskiego 3, 00-664 Warsaw, Poland, and Institute of Electronic Materials Technology, Wólczyńska 133, 01-919 Warsaw, Poland

Received January 15, 2007; Revised Manuscript Received March 29, 2007

ABSTRACT: Alternating linear and branched poly(*m*–*p*-anilines) and poly(*m*–*p*–*p*-anilines) have been synthesized via palladium-catalyzed amination reactions. Polymers were oxidized to radical cations either chemically or electrochemically. The presence of radical cations was manifested by the appearance of two and three new bands in the UV–vis–NIR spectra of poly(*m*–*p*-anilines) and poly(*m*–*p*–*p*-anilines), respectively. EPR spectra of frozen solutions of partially oxidized polymers confirmed the formation of high-spin states for all polymers studied.

Introduction

Recently the search for purely organic magnetic materials has attracted considerable attention. These types of materials should fulfill the following requirements: (i) they should show a very large *S* value, (ii) radicals or radical cations should exhibit sufficient chemical stability, (iii) organic molecules should be insensitive to spin defects. Considering the above reasons, oligoanilines or polyanilines containing alternating *m*–*p*-units seem to be very promising compounds as magnetic materials. They can show multiredox properties in which stable radical cations are generated.

Oligoanilines have been intensively investigated as typical high-spin systems. Janssen et al. have prepared *m*–*p*-aniline tetramers as well as linear and branched hexamers by the use of Ullmann condensation reaction with copper(I) iodide as a catalyst.^{1,2} However, the modeling and synthesis of anilines of different types have become very fruitful as a result of a spectacular progress in the formation of C–N bond by Pd-catalyzed amination reaction developed by Hartwig's³ and Buchwald's⁴ groups. Applying this route, Ito et al. have prepared amine dimer containing 1,3-benzene ring as spin coupling unit,⁵ whereas Selby and Blackstock have synthesized a dimer with 2,7-naphthalene coupling unit.⁶ Both dimers after partial oxidation showed a triplet ground state, which indicated a ferromagnetic interaction of spins. Similarly, a triplet state was also observed in the case of tetraaza[1,1,1,1]*m*–*p*–*m*–*p*-cyclophane oxidized to its radical cation form.⁷ One can suppose that star-shaped oligoanilines, which contain 1,3,5-benzenetriamine moiety can exhibit an increased *S* value. Thus, Tanaka's group has prepared new dendritic oligoarylamines^{8,9} exhibiting, in the oxidized form, dominant triplet and quartet states, as confirmed by pulsed ESR measurements.

To avoid the spin defects barriers molecules containing arylamines pendant groups have also been synthesized. Nishide et al. have obtained 3,4'-bis(diphenylamino)stilbene,¹⁰ in which an efficient spin exchange was realized by stilbene moiety. Similarly, *p*-phenylenediamine linked as pendant groups to 1,4-phenyleneethynylene and 1,4-phenylenevinylene synthesized by

Janssen et al.¹¹ showed ferromagnetic coupling of radical cations occurring by π -conjugated chains.

Considering ferromagnetic spins interactions, observed in discrete molecules, it seems very interesting to extend these studies by preparation of the corresponding macromolecular compounds of linear or branched type. However, to date such attempts were rather limited and no systematic studies concerning this subject have been performed. Goodson et al. have synthesized a series of poly(*m*-arylamines) and poly(*m*–*p*-arylamines),¹² but they have not focused on the magnetic properties of the obtained polymers. Intramolecular interactions of eight or nine spins were detected in the case of networked aromatic polyamines containing 1,3-disubstituted benzene as well as 1,3,5-trisubstituted benzene coupling units, prepared by Nishide et al.¹³ Similarly, according to magnetization measurements the spin value $S = 7/2$ was detected for hyperbranched poly[1,2(4)-phenylenevinyleneanilinium].¹⁴ Recently, we have prepared linear alternating poly(*m*–*p*-anilines) containing secondary and tertiary amine groups which after partial oxidation showed high-spin state.¹⁵

In this paper we report the synthesis of linear and branched polymers of aromatic amine type, which contain *m*–*p*- and *m*–*p*–*p*-units coupled to 1,3-benzene and 1,3,5-benzene rings, respectively. In the case of poly(*m*–*p*-anilines) a ferromagnetic interaction of spins coupled to *m*-phenylene can be expected similar to that observed for discrete molecules. However, in the case of poly(*m*–*p*–*p*-anilines) the spin interactions should be more complex and can be influenced by *p*-substituted as well as *m*-substituted benzene rings. Polymers were synthesized by the use of palladium-catalyzed amination of aryl bromides. Then, they were oxidized to radical cations either electrochemically or chemically. The formation of radical cations and the interactions of the generated spins were studied by UV–vis–NIR and EPR spectroscopies.

Experimental Section

Characterization Techniques. ¹H and ¹³C NMR spectra were recorded on a Varian Mercury (400 and 100 MHz) spectrometer and referenced with respect to TMS and solvents. IR spectra were monitored on Bio-RAD FTS-165 spectrometer using KBr pellets. UV–vis–NIR spectra were registered using a Cary 5000 (Varian) spectrometer. Electron spin resonance (ESR) experiments were

* Corresponding author. E-mail: ikulsz@ch.pw.edu.pl.

[†] Faculty of Chemistry, Warsaw University of Technology.

[‡] Institute of Electronic Materials Technology.

carried out with a Bruker ESP-300 spectrometer with 100 kHz field modulation and phase-sensitive detection, which operated at a microwave frequency of about 9.4 GHz (X-band). Saturation of the ESR signal was avoided by using low microwave power, i.e., 0.2 mW for the $\Delta M_s = \pm 1$ transition and 2 mW for the $\Delta M_s = \pm 2$ transition. Mass spectra were measured by the EI method on an AMD 604 mass spectrometer. Molecular weights were determined by size exclusion chromatography (SEC) on a LAB Alliance chromatograph equipped with a column Jordi Gel DVB Mixed Bed. All synthesized compounds studied were subject to C, H and N elemental combustion analysis. Cyclic voltammograms were recorded using an Autolab potentiostat (Eco Chimie).

Reagents. 1,4-Phenylenediamine, 1-bromo-4-butylbenzene, 1-bromo-4-*tert*-butylbenzene, 1,3-dibromobenzene, 1,3,5-tribromobenzene, palladium acetate, (Pd(OAc)₂), 2,2'-bis(diphenylphosphino)-1,1'-binaphthyl, (BINAP), tris-*tert*-butylphosphine, (*t*-Bu₃P), sodium *tert*-butoxide, (*t*-BuONa), trifluoroacetic acid, (TFA), 3-chloroperbenzoic acid, (CPB), nitronium tetrafluoroborate, NO₂BF₄, *N,N*-dimethylformamide, (DMF), anhydrous acetonitrile, diphenylamine, and 4-butylaniline were purchased from Aldrich. Bu₄NBF₄ was purchased from Fluka. Diphenylamine was purified by a liquid chromatography using CH₂Cl₂/ethyl acetate (20:1). 4-Butylaniline was distilled under reduced pressure. *N*-Bromosuccinimide (NBS) was crystallized from water.

Monomers Synthesis. All glassware was oven dried, assembled hot, and cooled under a dry argon stream before use. All reactions were performed under dry argon.

***N,N'*-Bis(4-butylphenyl)-1,4-phenylenediamine (1).** 1,4-Phenylenediamine, 0.815 g (7.5 mmol), 1-bromo-4-butylbenzene, 3.51 g (16.5 mmol), sodium *tert*-butoxide, 1.8 g (18.75 mmol), palladium acetate, 84.2 mg (0.375 mmol), and BINAP, 0.7 g (1.125 mL), were dissolved in 15 mL of dry toluene under an argon atmosphere. The reaction mixture was stirred and heated at 110 °C for 12 h. The reaction mixture was then cooled to room temperature and washed with 30 mL of distilled water. The aqueous phase was extracted with three 5 mL portions of diethyl ether. The organic layers were combined and dried over MgSO₄. Removal of the solvents followed by chromatography on silica gel (CHCl₃/hexanes, 2:1) resulted in an off-white solid. The resulting solid was recrystallized from ethyl acetate/hexanes to give 1.94 g (5.20 mmol, 69.3% yield) of (**1**) as white, shiny plates. Mp: 121–123 °C. ¹H NMR (400 MHz, C₆D₆), δ : 7.01 (d, *J* = 8.4 Hz, 4H), 6.87–6.83 (m, 8H), 4.90 (s, 2H), 2.49 (t, *J* = 7.6 Hz, 4H), 1.57–1.50 (m, 4H), 1.34–1.25 (m, 4H), 0.88 (t, *J* = 7.2 Hz, 6H). ¹³C NMR (100 MHz, C₆D₆), δ : 142.7, 137.9, 134.6, 129.5, 120.5, 117.3, 35.3, 34.3, 22.6, 14.2. IR (cm⁻¹): 3396, 3358, 3026, 2956, 2925, 2855, 1613, 1529, 1516, 1461, 1312, 1226, 1108, 817. Anal. Calcd for C₂₆H₃₂N₂: C, 83.87; H, 8.60; N, 7.53. Found: C, 83.97; H, 8.54; N, 7.47. *M*⁺/*z* = 372.4

Diphenyl-(4-*tert*-butylphenyl)amine (3). Palladium acetate, 63.4 mg (0.24 mmol), and *t*-Bu₃P, 153.4 mg (0.76 mmol), were dissolved in 2 mL of dry toluene under argon atmosphere and stirred at room temperature for 0.5 h. Then 1-bromo-4-*t*-butylbenzene, 2.044 g (9.6 mmol), diphenylamine, 1.352 g (8 mmol), sodium *tert*-butoxide, 1.152 g (12 mmol), and toluene, ca. 18 mL, were added to the reaction flask. The mixture was stirred and heated at 110 °C for 4 h. After the mixture was cooled to room temperature, water (30 mL) was added and the organic layer separated. The remaining aqueous layer was then extracted with diethyl ether (3 × 5 mL). The combined organic fractions were dried over MgSO₄. The crude product was purified by chromatography on silica gel eluting with hexanes/CH₂Cl₂ (2:1) and then recrystallized in hexanes to give 2.27 g (7.54 mmol, 94.3% yield) of (**3**) as white plates. Mp: 98.6–99.0 °C. ¹H NMR (400 MHz, CDCl₃), δ : 7.27–7.21 (m, 6H), 7.10–7.07 (m, 4H), 7.03–6.96 (m, 4H), 1.31 (s, 9H). ¹³C NMR (100 MHz, CDCl₃), δ : 148.0, 145.7, 145.0, 129.1, 126.0, 124.0, 123.8, 122.3, 34.3, 31.4. IR (cm⁻¹): 3058, 3036, 2960, 2866, 1593, 1586, 1513, 1492, 1384, 1282, 835, 751, 695. Anal. Calcd for C₂₂H₂₃N: C, 87.71; H, 7.64; N, 4.65. Found: C, 87.05; H, 7.96; N, 4.44.

Di(4-bromophenyl)-(4'-*tert*butylphenyl)amine (4). Amine **3**, 1.135 g (3.77 mmol), was dissolved in 10 mL of dry DMF under argon atmosphere. NBS, 1.48 g (8.295 mmol), was dissolved in 10 mL of dry DMF and placed in a funnel. The solution of NBS was added dropwise from a funnel to the solution of amine **3** stirred at room temperature. After 1 h of stirring, 50 mL of distilled water was added to form an emulsion which was extracted with three 10 mL portions of diethyl ether. The combined organic layers were washed with brine, then with water and dried over MgSO₄. The crude product was recrystallized from 2-propanol to give 1.4 g (3.05 mmol, 80.9% yield) of white powder. Mp: 108.4–108.5 °C. ¹H NMR (400 MHz, CDCl₃), δ : 7.34–7.31 (m, 2H), 7.28–7.26 (m, 4H), 7.00–6.96 (m, 2H), 6.95–6.91 (m, 4H), 1.31 (s, 9H). ¹³C NMR (100 MHz, C₆D₆), δ : 147.0, 146.9, 144.7, 132.6, 126.7, 125.4, 123.9, 115.4, 34.3, 31.4. IR (cm⁻¹): 3062, 3033, 2960, 2866, 1578, 1513, 1485, 1363, 1312, 1269, 1105, 1070, 1006, 819. Anal. Calcd for C₂₂H₂₁Br₂N: C, 57.54; H, 4.58; Br, 34.83; N, 3.05. Found: C, 57.36; H, 4.79; Br 33.86; N, 3.02.

Bis[(4'-butylphenyl)-4-aminophenyl]-4''-*tert*-butylphenylamine (2). The same procedure as for preparation of amine **3** was used. Palladium acetate, 67.2 mg (0.3 mmol), and BINAP, 0.559 g (0.9 mmol), were dissolved in 2 mL of dry toluene. Then compound **4** (2.295 g, 5 mmol), 4-butylaniline (1.63 g, 10.94 mmol), sodium *tert*-butoxide (1.43 g, 14.9 mmol), and 15 mL of dry toluene were added to the reaction flask. The mixture was stirred and heated at 110 °C for 4 h under an argon atmosphere. The crude product was chromatographed on silica gel eluting with CH₂Cl₂/hexanes (2:1) and then crystallized in ethyl acetate/hexanes to give 1.74 g (2.92 mmol) of (**2**) as a white powder. The reaction yield was 58.5%. Mp: 117.5–119.0 °C. ¹H NMR (400 MHz, C₆D₆), δ : 7.23 (s, 4H), 7.14–7.12 (m, 4H), 7.00–6.98 (m, 4H), 6.88–6.86 (m, 4H), 6.81–6.79 (m, 4H), 4.92 (s, 2H), 2.48 (t, *J* = 7.6 Hz, 4H), 1.56–1.48 (m, 4H), 1.33–1.26 (m, 4H), 1.25 (s, 9H), 0.87 (t, *J* = 7.4 Hz, 6 Hz). ¹³C NMR (100 MHz, C₆D₆), δ : 142.1, 139.2, 135.1, 129.5, 126.3, 125.9, 122.6, 119.2, 118.1, 35.3, 34.2, 31.6, 22.6, 14.1. IR (cm⁻¹): 3389, 3032, 2958, 2926, 2870, 1615, 1506, 1313, 1271, 823. Anal. Calcd for C₄₂H₄₉N₃: C, 84.70; H, 8.24; N, 7.06. Found: C, 84.65; H, 8.15; N, 7.07. *M*⁺/*z* = 595.5.

General Polymerization Procedure. Polycondensation has been done according to the method of Goodson et al.¹² In the case of linear polymers (**PA1**, **PA2**) 11.2 mg (0.05 mmol) of Pd(OAc)₂ and 30.3 mg (0.15 mmol) of *t*-Bu₃P were weighed in a glove bag under an argon atmosphere, mixed with 3 mL of dry toluene and stirred for 15 min. Then 2.5 mmol of 1,3-dibromobenzene, 2.5 mmol of diamine, 7.5 mmol of sodium *tert*-butoxide, and 12 mL of toluene were placed in a reaction flask containing the catalyst under an argon atmosphere. The mixture was stirred and heated at 90 °C for 4 days.

In the case of branched polymers (**PAB1**, **PAB2**), 6.7 mg (0.03 mmol) of Pd(OAc)₂, 18.2 mg (0.09 mmol) of *t*-Bu₃P and 3 mL of toluene were placed in a reaction flask under an argon atmosphere. After 15 min of stirring, 1.5 mmol of diamine, 1.0 mmol of 1,3,5-tribromobenzene, 4.5 mmol of sodium *tert*-butoxide, and 12 mL of dry toluene were added to the flask. To minimize the formation of gel, the mixture was stirred and heated at 90 °C for 1 day in the case of **PAB1** and for 2 days to obtain **PAB2**.

The crude mixture was cooled to room temperature and a polymer was precipitated by transferring the solution into 300 mL of methanol by a pipet. The solid was isolated via filtration, washed with water and methanol. Low-molecular weight products were removed by extraction with acetone and then with hexanes. After their removal the polymer was dissolved in a small amount of toluene, then precipitated in methanol, filtered, and finally dried in a vacuum.

PA1. The resulting polymer was isolated as gray-white powder (0.92 g, the polymerization yield 82.5%). ¹H NMR (400 MHz, CDCl₃) δ : 6.99–6.91 (m, 9H), 6.90 (s, 4H), 6.80 (s, 1H), 6.54 (d, *J* = 8 Hz, 2H), 2.50 (t, *J* = 7.4 Hz, 4H), 1.57–1.50 (m, 4H), 1.37–1.28 (m, 4H), 0.89 (t, *J* = 7.2 Hz, 6 H). ¹³C NMR (100 MHz, CDCl₃) δ : 148.5, 145.0, 142.5, 137.1, 128.9, 125.7, 125.0, 124.8, 124.0, 116.8, 35.0, 33.6, 22.4, 14.0. IR (cm⁻¹): 3447, 3026, 2967,

2955, 2870, 2856, 1590, 1503, 1481, 1264, 1242, 827, 772, 695. Anal. Calcd for $[(C_{32}H_{34}N_2) \cdot (H_2O)_{0.36}]_n$: C, 84.87; H, 7.67; N, 6.19. Found: C, 84.79; H, 7.64; N, 6.14.

In the low-molecular weight fraction extracted from the crude polycondensation product the presence of a cyclic product (ca. 15 wt %), namely tetraaza[1.1.1.1]*m-p-m-p*-cyclophane, $(C_{64}H_{68}N_4)_n$, was detected. 1H NMR (400 MHz, C_6D_6), δ : 7.29–7.26 (m, 8H), 6.96–6.94 (m, 8H), 6.91 (t, J = 8.0 Hz, 2H), 6.86 (s, 8H), 6.78 (dd, J = 8.0 Hz, 2.4 Hz, 4H), 6.68 (t, J = 2.2 Hz, 2H), 2.43 (t, J = 7.6 Hz, 8H), 1.51–1.43 (m, 8H), 1.23–1.20 (m, 8H), 0.84 (t, J = 7.4 Hz, 12H). ^{13}C NMR (100 MHz, C_6D_6), δ : 149.8, 145.4, 143.3, 137.8, 129.9, 129.6, 126.2, 125.5, 116.0, 115.0, 35.4, 34.1, 22.7, 14.1. M^+/z = 892.3.

PA2. The resulting polymer was isolated as an off-white powder (1.05 g, the polymerization yield 62.8%). 1H NMR (400 MHz, $CDCl_3$), δ : 6.98–6.94 (m, 13H), 6.92 (s, 8H), 6.81 (s, 1H), 6.57 (dd, J = 8.0 Hz, 2.0 Hz, 2H), 2.49 (t, J = 7.4 Hz, 4H), 1.55–1.51 (m, 4H), 1.32–1.27 (m, 13H), 0.89 (t, J = 7.2 Hz, 6H). ^{13}C NMR (100 MHz, $CDCl_3$), δ : 148.7, 145.2, 142.8, 142.2, 137.0, 129.2, 128.9, 125.9, 125.2, 124.7, 123.8, 122.9, 116.5, 35.0, 33.7, 31.4, 22.4, 14.0. IR (cm^{-1}): 3435, 3032, 2955, 2927, 2857, 1591, 1500, 1482, 1312, 1263, 826, 774, 696. Anal. Calcd for $[(C_{48}H_{51}N_3) \cdot (H_2O)_{0.81}]_n$: C, 84.26; H, 7.70; N, 6.14. Found: C, 83.58; H, 7.36; N, 6.05.

PAB1. The resulting polymer was isolated as a gray-white powder (0.46 g of gel, i.e., 74 wt %, chloroform soluble fraction 0.16 g, i.e., 26 wt %). 1H NMR (400 MHz, $CDCl_3$), δ : 7.00–6.90 (m, 16H), 6.85 (s, 8H), 6.33 (s, 2H), 5.87 (s, 1H), 2.47 (m, 8H), 1.59–1.42 (m, 8H), 1.38–1.24 (m, 8H), 0.92–0.85 (m, 12H). ^{13}C NMR (100 MHz, $CDCl_3$), δ : 150.2, 145.0, 143.4, 137.7, 129.4, 129.3, 126.6, 125.3, 35.4, 33.9, 22.7, 14.2. IR (cm^{-1}) 3435, 3026, 2955, 2926, 2856, 1586, 1503, 1456, 1276, 1244, 828, 697. Anal. Calcd for $(C_{45}H_{48}N_3)_n$: C, 85.71; H, 7.62; N, 6.67. Found: C, 84.64; H, 7.52; N, 6.54.

PAB2. The resulting polymer was isolated as an off-white powder (0.54 g of crude polymer, chloroform soluble fraction 0.28 g, 52.1 wt %). 1H NMR (400 MHz, $CDCl_3$), δ : 6.96–6.84 (m, 20H), 6.43 (s, 1H), 6.34 (s, 1H), 6.26 (s, 1H), 2.52–2.42 (m, 4H), 1.58–1.46 (m, 4H), 1.38–1.20 (m, 13H), 0.98–0.82 (m, 6H). ^{13}C NMR (100 MHz, $CDCl_3$), δ : 148.6, 144.4, 142.5, 141.3, 137.2, 129.0, 128.8, 125.8, 124.6, 124.3, 122.8, 35.0, 33.6, 31.4, 22.4, 14.0. IR (cm^{-1}): 3401, 3032, 2955, 2927, 2857, 1586, 1500, 1456, 1310, 1266, 1247, 828. Anal. Calcd for $(C_{69}H_{73.5}N_{4.5})_n$: C, 85.85; H, 7.62; N, 6.53. Found: C, 84.81; H, 7.53; N, 6.50.

Oxidation Procedure. The electrochemical oxidation was monitored by cyclic voltammetry. For these investigations polymers were dissolved in CH_2Cl_2 (10^{-3} M). The experiments were carried out in a one compartment electrochemical cell, in a solution of 0.1 M Bu_4NBF_4 in CH_2Cl_2 with $Ag/0.1$ M $AgNO_3$ in acetonitrile as a reference electrode and a Pt counter electrode. Scan rate was 50 mV/s. The surface of the Pt disk electrode was 3 mm².

In the chemical oxidation, two types of oxidants were used: nitronium tetrafluoroborate which is a one-electron oxidizing agent and 3-chloroperbenzoic acid, CPB—a two-electron oxidizing agent.

The chemical oxidation reaction was carried out in an argon atmosphere. In a typical procedure 0.03 mmol of polymer was dissolved in 1.5 mL of CH_2Cl_2 and oxidized with 0.03 mmol of NO_2BF_4 in 1 mL of the same solvent or polymer was dissolved in CH_2Cl_2/TFA (9:1) solution and then oxidized with 0.015 mmol of CPB in 1 mL of CH_2Cl_2 . These solutions of oxidized polymers were used directly for EPR measurements.

For quantitative UV–vis–NIR studies the solution of **PA1** ($c = 2 \times 10^{-3}$ M) and **PA2** ($c = 2 \times 10^{-3}$ M) in CH_2Cl_2/TFA (9:1) were oxidized with CPB in CH_2Cl_2 ($c = 9.5 \times 10^{-4}$ M). The real content of CPB in commercial product was determined by titration ($I^-/S_2O_3^{2-}$). 1 mL of polymer solution was mixed with appropriate volume of CPB solution and diluted to an overall volume of 3 mL with CH_2Cl_2/TFA (9:1). Then, 0.2 mL of this oxidized polymer solution was additionally diluted with 2.3 mL of CH_2Cl_2/TFA (9:1) and the UV–vis–NIR spectrum was measured.

Results and Discussion

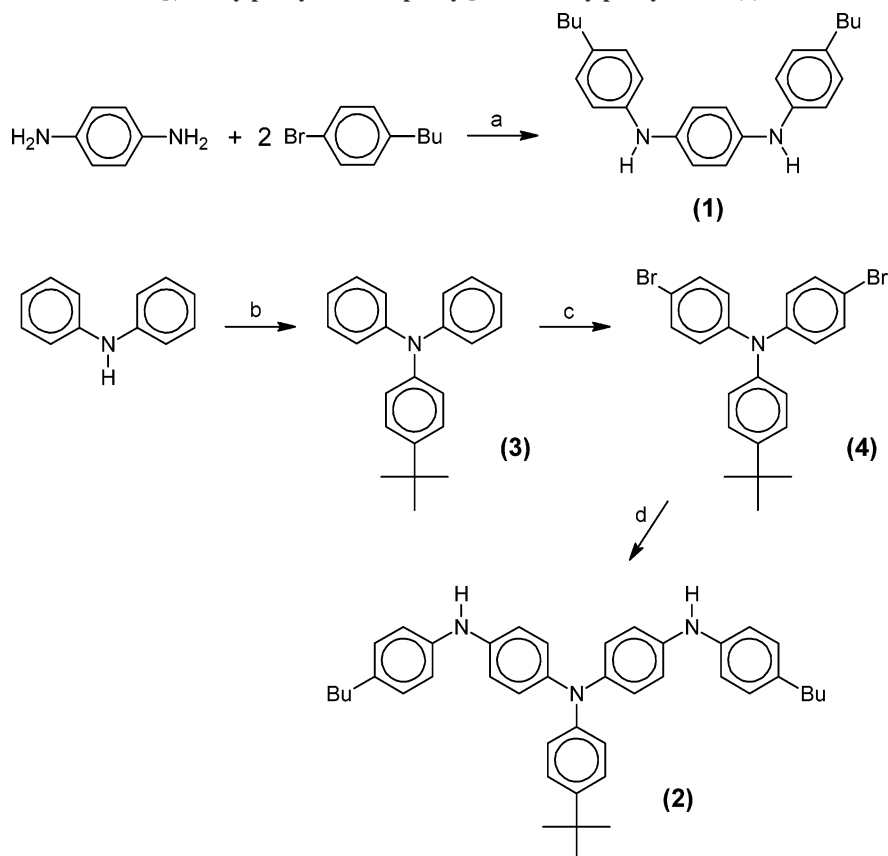
Oligoaniline derivatives coupled to *m*-benzene have been recommended as stable high-spin molecules. In an attempt to extend the family of magnetic organic materials to macromolecular compounds of aromatic amine type we have synthesized new amines, namely *N,N'*-bis(4-butylphenyl)-1,4-phenylenediamine (**1**) and bis[(4'-butylphenyl)-4-aminophenyl]-4'-*tert*-butylphenylamine (**2**) by the use of palladium catalyzed amination reactions (Scheme 1), capable of undergoing the condensation reaction with bromoderivatives of benzene. Amine **1** was prepared from *p*-phenylenediamine and 4-butylbromobenzene with a yield of 69.3%. Amine **2** was synthesized in a three-step reaction. First, diphenylamine reacted with bromo-4-*tert*-butylbenzene to form **3**. Amine **3** was brominated using NBS and then reacted with 4-butylaniline to obtain amine **2** with the yield of 57.6% after recrystallization. Polycondensations between amines **1** or **2** and 1,3-dibromobenzene lead to linear polymers **PA1** and **PA2** whereas their reactions with 1,3,5-tribromobenzene result in branched polymers **PAB1** and **PAB2** (Scheme 2).

Macromolecular parameters of the obtained polycondensation products are listed in Table 1. In the case of **PA1** the polycondensation reaction yield with respect to the fraction insoluble in hexane was ca. 50 wt % of obtained crude polymer. It can be related to the formation of cyclic oligomers, which was facilitated in the presence of *m*-substituted reagent. This is evidenced by the presence of tetraaza[1.1.1.1]*m-p-m-p*-cyclophane as the major component of the extracted low-molecular weight fraction.

The problem of cyclization was less important in the case of polymer **PA2** containing *m-p-p*-units where the hexane insoluble fraction constituted 67.5 wt % of prepared crude polymer. It is evident that the use of *p*-substituted reactants prevents from easy cyclization, which was detected for **PA1**. In the cases of branched polymers **PAB1** and **PAB2** facile gelation took place, as expected. Thus, we reduced the polycondensation time to 1 and 2 days, respectively. In these conditions polymer **PAB1** formed 74 wt % of gel and 26 wt % of chloroform soluble fraction, whereas polymer **PAB2** was separated into 20.5 wt % of gel, 27.4 wt % of hexanes soluble fraction, and 52.1 wt % of chloroform soluble fraction.

As it has already been stated, the synthesized polymers can be oxidized to radical cations either chemically or electrochemically. If the latter process is carried out in the cyclic voltammetry configuration, characteristic oxidation waves corresponding to the consecutive electron abstraction appear accompanied by the corresponding reduction waves (Figure 1). **PA1** shows the most resolved voltammogram of all polymers studied. In its oxidative part three anodic peaks can be distinguished at $E_{ox1} = 0.22$ V, $E_{ox2} = 0.45$ V and $E_{ox3} \approx 0.88$ V (Figure 1a) i.e., at the potential values which are close to those observed by Goodson et al.¹² for polyamines of similar chemical nature. Similar voltammograms are also registered for aromatic amine oligomers which, to some extent, can be considered as model compounds of the polymers studied in this research.^{1,5} By comparison with these data, we are tempted to interpret the first two anodic peaks in the cyclic voltammogram of **PA1** as related to the removal of first and second electrons from two neighboring *p*-phenylenediamine moieties. These two redox couples are reversible, as far as the polymer charging/discharging processes are concerned, since the amount of charge used for the oxidation of **PA1** is, within an experimental error, equal to that recovered during its cathodic reduction to the neutral state. However, the measured peak to peak separation is 80 mV which is by ca. 20 mV larger

Scheme 1. Syntheses of *N,N'*-Bis(4-butylphenyl)-1,4-phenylenediamine (**1**) and Bis[(4'-butylphenyl-4-aminophenyl)-4''-*tert*-butylphenylamine (**2**)^a



^a Key: (a) Pd(OAc)₂, BINAP, *t*-BuONa, toluene, 110 °C; (b) 1-bromo-4-*tert*-butylbenzene, Pd(OAc)₂, *t*-Bu₃P, *t*-BuONa, toluene, 110 °C; (c) NBS, DMF; (d) 4-butylaniline, Pd(OAc)₂, BINAP, *t*-BuONa, toluene, 110 °C.

than the theoretical value expected for a one electron redox process. Several factors can contribute to this discrepancy like ohmic drop and others. One electron process must inevitably lead to the formation of a radical cation. Unequivocal verification whether stable radical cations are formed during the first two redox processes requires the determination of the charge-spin relationship in a specially designed EPR spectroelectrochemical experiment.¹⁶ Such studies are planned in the near future. The third wave can arise from the multielectron process leading to the formation of dication states (all imine nitrogens). This is frequently accompanied by deprotonation which results in a more irreversible character of the third redox couple, at least in electrolytes which do not contain a source of protons.

In the case of the voltammogram of **PA2** (Figure 1b), in the potential range from -0.2 to +0.8 V, two anodic peaks were observed at 0.29 V (with a shoulder at ca. 0.12 V) and 0.60 V, each of them has its cathodic counterpart. The couples are reversible in the chemical sense since again the integration of the anodic and cathodic currents gives roughly the same result. The values of the $E_{ox} - E_{red}$ separations were equal to 130 and 140 mV. The verification whether the observed differences originate from two (or more) electron redox processes or from merging of two one-electron redox couples, which in this case remain unresolved, requires additional studies.

The voltammogram of **PAB1** resembles that of its linear analogue (**PA1**), however, it is less reversible and its redox couples are very poorly resolved (Figure 1c). The same applies to the comparison of **PA2** and **PAB2** (Figure 1d). This is not unexpected taking into account the branched nature of these polymers leading to energetically nonequivalent segments. Similar poorly resolved voltammogram was reported by Michi-

nobu et al.¹³ for branched polyarylamines. We can conclude that the presence of 1,3,5-trisubstituted benzene rings in the polymer **PAB1** and **PAB2** did not allow the detection of the discrete oxidation states. Moreover, similar effect was observed in the cases of 1,3,5-benzenetriamine model compounds studied by Ito et al.⁸ and Hirao et al.⁹

The chemical oxidation led also to the formation of radical cations. This process can be investigated by the registration of the changes in the UV-vis-NIR polymers spectra induced by their titration with an appropriate oxidizing agent. We have carried out such titration studies in neutral and acidic media using NO₂BF₄ and *m*-chloroperbenzoic acid (CPB) as oxidants, respectively. The UV-vis-NIR spectrum of polymer **PA1** in neutral medium (CH₂Cl₂) shows one band at 318 nm ($\epsilon = 3.4 \times 10^4 \text{ M}^{-1} \text{ cm}^{-1}$), which can be attributed to the $\pi-\pi^*$ transition in the phenylene ring (Figure 2a). Upon stepwise addition of the oxidant, new bands appear at 427 and 870 nm (radical cations bands) and grow in intensity with simultaneous decrease of the $\pi-\pi^*$ transition band intensity. The highest intensities of these bands correspond to the theoretical oxidation of half-amount of nitrogens to radical cations **PA1**^{•+}. The positions of the bands shift slightly from 427 to 410 nm and from 870 to 860 nm. Well-defined isosbestic point can be observed at 352 nm proving that only two optically different phases are present (neutral and radical cation one) which mutually interconvert.

The oxidation of polymer **PA1** in acidic medium (TFA/CH₂-Cl₂, 1:9) proceeds similarly (Figure 2b), although the positions of the bands characteristic of the radical cations are shifted to higher wavelengths as compared to the case of the neutral medium. The band observed at 895 nm for low oxidation states

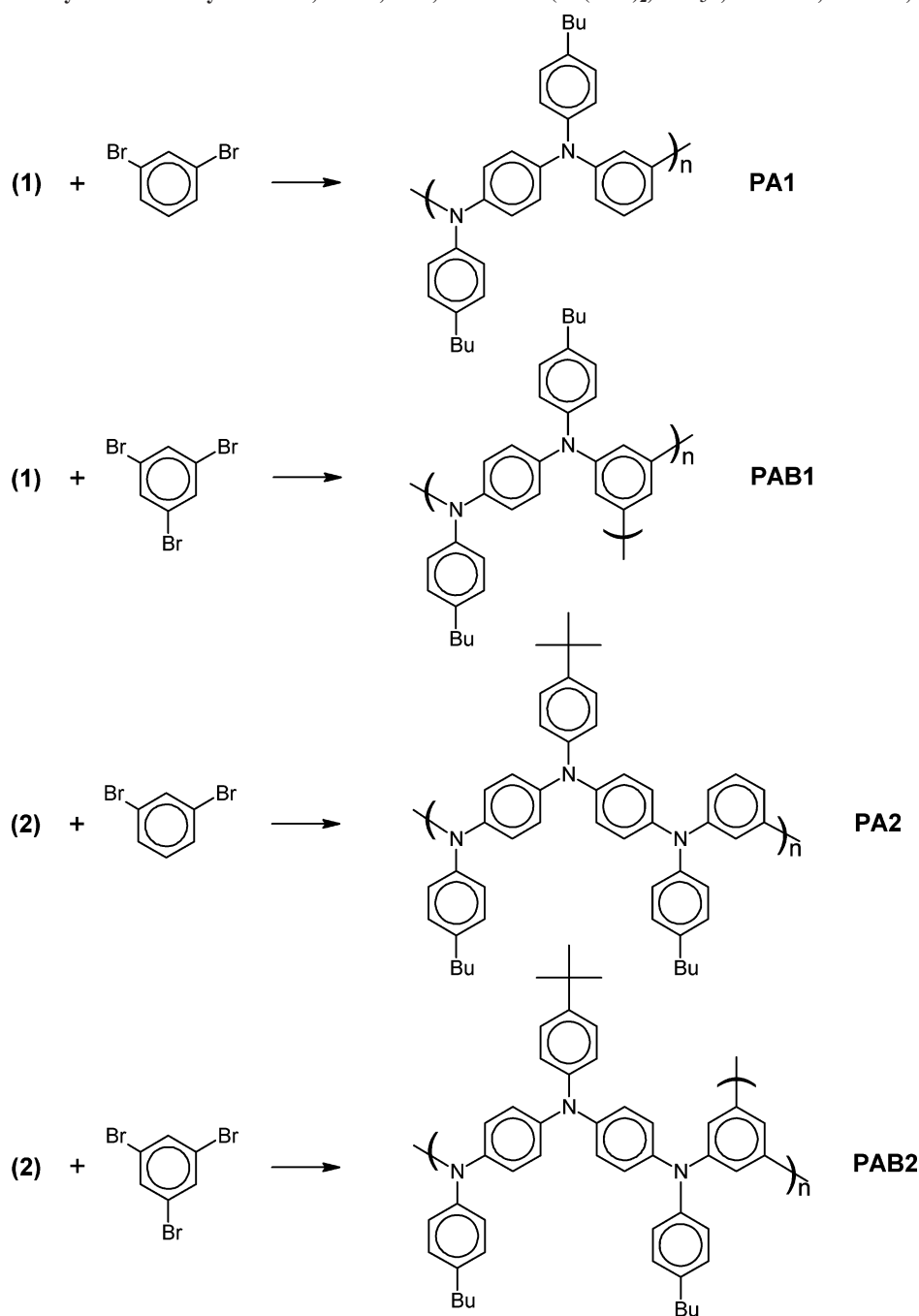
Scheme 2. Syntheses of Polymers PA1, PAB1, PA2, and PAB2 ($\text{Pd}(\text{OAc})_2$, $t\text{-Bu}_3\text{P}$, $t\text{-BuONa}$, Toluene, 90 °C)

Table 1. Molecular Weights of Polymers PA1, PA2, PAB1, and PAB2 Determined by SEC Measurements

polymer	M_n [Da $\times 10^{-4}$]	M_w [Da $\times 10^{-4}$]	M_p [Da $\times 10^{-4}$]	D
PA1	2.2	3.6	2.8	1.6
PAB1	0.8	1.6	1.1	2.0
PA2	2.8	13.6	6.0	4.9
PAB2	1.1	1.9	1.6	1.7

Notes: determined in CHCl_3

is displaced to 990 nm ($\epsilon = 1.8 \times 10^4 \text{ M}^{-1} \text{ cm}^{-1}$) for the **PA1**⁺ state, whereas the band at 419 nm ($\epsilon = 2.3 \times 10^4 \text{ M}^{-1} \text{ cm}^{-1}$) does not change its initial position. Further oxidation causes the appearance of a new band at 702 nm and a decrease in the intensity of the radical cation's bands. The band at 702 nm can be attributed to the formation of dications in the *p*-phenylenediamine unit. Figure 2d shows the dependence of absorbance measured for the π - π^* transition band and the radical cations

peaks vs the theoretical number of electrons removed from polymer unit.

The oxidation of branched **PAB1** in acidic medium ($\text{TFA}/\text{CH}_2\text{Cl}_2$, 1:9) is similar to that of **PA1** (Figure 2c). In the UV-vis-NIR spectra the bands characteristic of radical cations appeared at 419 ($\epsilon = 2.2 \times 10^4 \text{ M}^{-1} \text{ cm}^{-1}$) and 968 nm ($\epsilon = 1.6 \times 10^4 \text{ M}^{-1} \text{ cm}^{-1}$).

The UV-vis-NIR spectrum of **PA2** in CH_2Cl_2 shows only one band at 323 nm ($\epsilon = 4.4 \times 10^4 \text{ M}^{-1} \text{ cm}^{-1}$) (π - π^* transition, Figure 3a). It is evident that the conjugation in the case of **PA2** is higher than that in **PA1**. The oxidation of **PA2** is manifested by the appearance of three new bands at 439, 730, and 1290 nm. Further oxidation causes a significant displacement of the 1290 nm band to 1170 nm. The band at 439 nm shifts to 416 nm, whereas the band at ca. 730 nm does not change its initial position. The presence of three new bands can

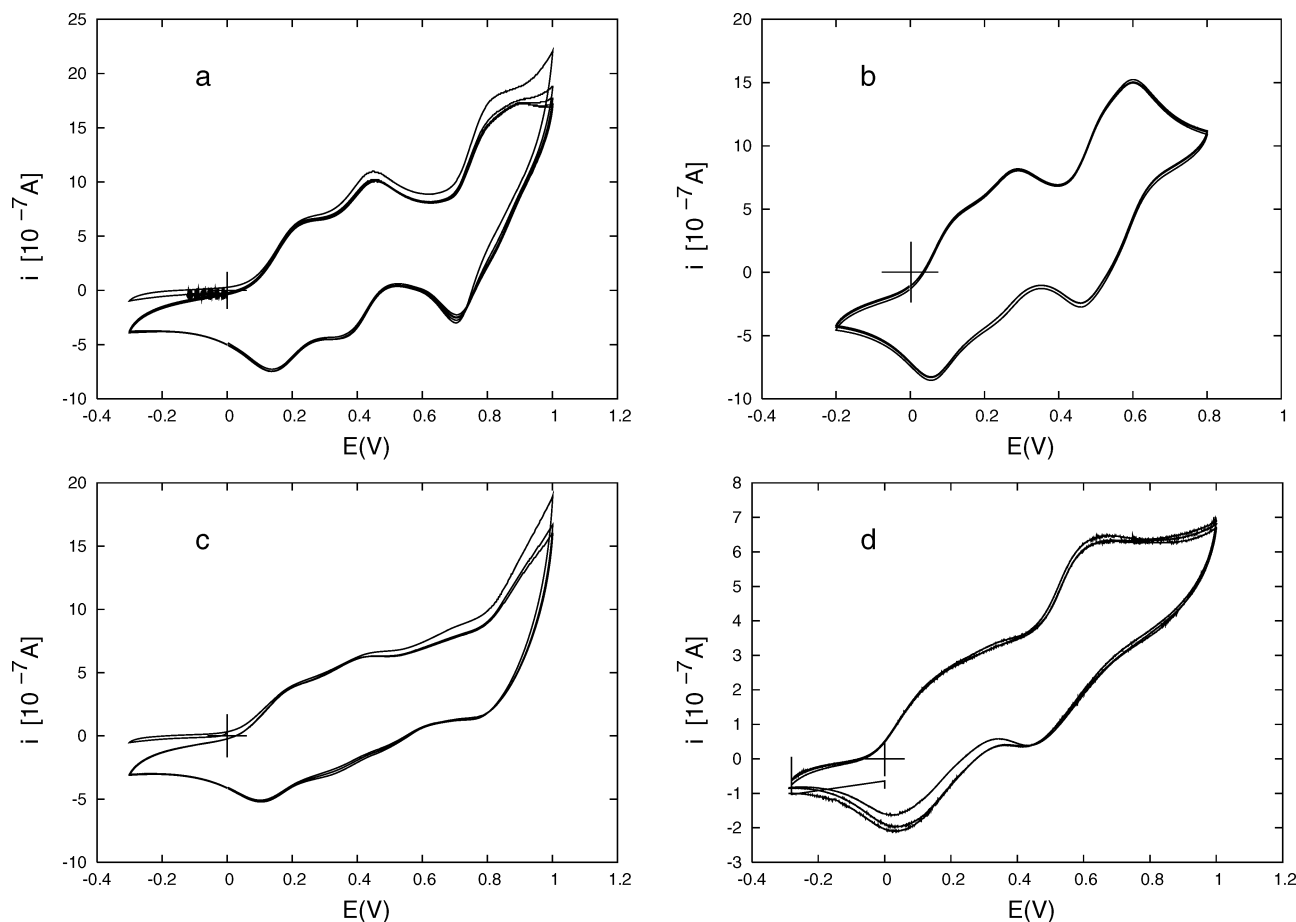


Figure 1. Cyclic voltammograms (four consecutive scans) obtained for polymers in CH_2Cl_2 solution ($c = 10^{-3}$ M) containing an electrolyte—0.1 M Bu_4NBF_4 , (reference electrode— $\text{Ag}/0.1$ M AgNO_3 in acetonitrile): (a) **PA1**; (b) **PA2**; (c) **PAB1**; (d) **PAB2**. Scan rate: 50 mV/s.

Table 2. EPR Parameters of the Spectra of Oxidized Polyanilines

sample ^a	$\Delta M_s = \pm 1$		$\Delta M_s = \pm 2$	
	<i>g</i>	ΔB_{pp} [mT]	<i>g</i>	ΔB_{pp} [mT]
PA1 ¹⁺	2.003	0.6	4.004	0.9
PAB1 ³⁺	2.003	0.8	4.001	0.8
PA2 ²⁺ , sample a	2.003	0.9		
PA2 ²⁺ , sample b	2.003	0.8	4.004	1.1
PAB2 ²⁺	2.002	0.5	4.004	1.2

^a Abbreviations in column 1 denote the formal oxidation state of the polymer repeat unit calculated from the oxidant to polymer molar ratio. It is assumed that the oxidation results in the creation of radical cations without their consecutive recombination to spinless dications.

be related to the nonequivalent structures of radical cations located mostly on first or second nitrogen atoms in the *p*-phenylene-*p*-phenylene unit. Similarly as in the case of **PA1** an isosbestic point is observed at 360 nm. **PA2** was also oxidized in acidic medium ($\text{TFA}/\text{CH}_2\text{Cl}_2$, 1:9). The general features of the UV-vis-NIR spectra (Figure 3b) are similar to that presented above for the oxidation of **PA1**. However, the detailed inspection of the positions and the shapes of the bands characteristic of the radical cations reveals significant differences. Spectrum 1 corresponds to the theoretical removal of one electron from two neighboring *p*-phenylene-*p*-phenylene units. The bands are located at 433 ($\epsilon = 2.6 \times 10^4 \text{ M}^{-1} \text{ cm}^{-1}$), 753 ($\epsilon = 1.7 \times 10^4 \text{ M}^{-1} \text{ cm}^{-1}$), and 1266 ($\epsilon = 2.2 \times 10^4 \text{ M}^{-1} \text{ cm}^{-1}$) nm. The NIR band is nearly symmetric. Further oxidation changes the shape of the NIR band. In spectrum 2 (removal of 2 electrons from two neighboring units), the NIR band becomes asymmetric with a maximum located at 1015 nm. Further removal of 3 and 4 electrons from two neighboring units (spectra 3 and 4) leads to the spectra which show an increase in the

intensity of the high-energy component of the NIR band. The maximum is shifted to 985 and then 958 nm. Figure 3d shows the dependence of the absorbance measured for the radical cations and dications peaks vs the theoretical number of electrons removed from polymer unit. Comparing the UV-vis-NIR spectra of **PA2** oxidized in neutral and acidic media we can conclude that the radical cations are more localized in the polymer in contact with the acidic medium than with the neutral one, which is caused, in the former, by the protonation of aniline nitrogens. The oxidation of polymer **PAB2** causes similar changes in the UV-vis-NIR spectra as those observed for **PA2**. However, the bands in the NIR region are located at lower energies as compared to the spectra of **PA2**; i.e., at 434 ($\epsilon = 2.6 \times 10^4 \text{ M}^{-1} \text{ cm}^{-1}$), 770, ca.1000 and 1190 ($\epsilon = 2.5 \times 10^4 \text{ M}^{-1} \text{ cm}^{-1}$) nm.

The main differences in the character of UV-vis-NIR spectra are related to the length of para-conjugated segments. The UV-vis-NIR spectra of the polymers synthesized using the same amines are similar and little dependent on the macromolecule topology (linear or branched). Small differences of the spectra of linear and branched polymers of the same type can be probably related to the variations in the geometrical distortion induced by 1,3-disubstituted or 1,3,5-trisubstituted benzene rings.

The interactions of radical cations generated by chemical oxidation of the polymers studied were investigated using ESR spectroscopy. In all cases polymers were oxidized to radical cations in acidic medium ($\text{CH}_2\text{Cl}_2/\text{TFA}$, 9:1) with CPB as an oxidizing agent. The EPR parameters of the spectra of polymers oxidized to different oxidation states are listed in Table 2. It

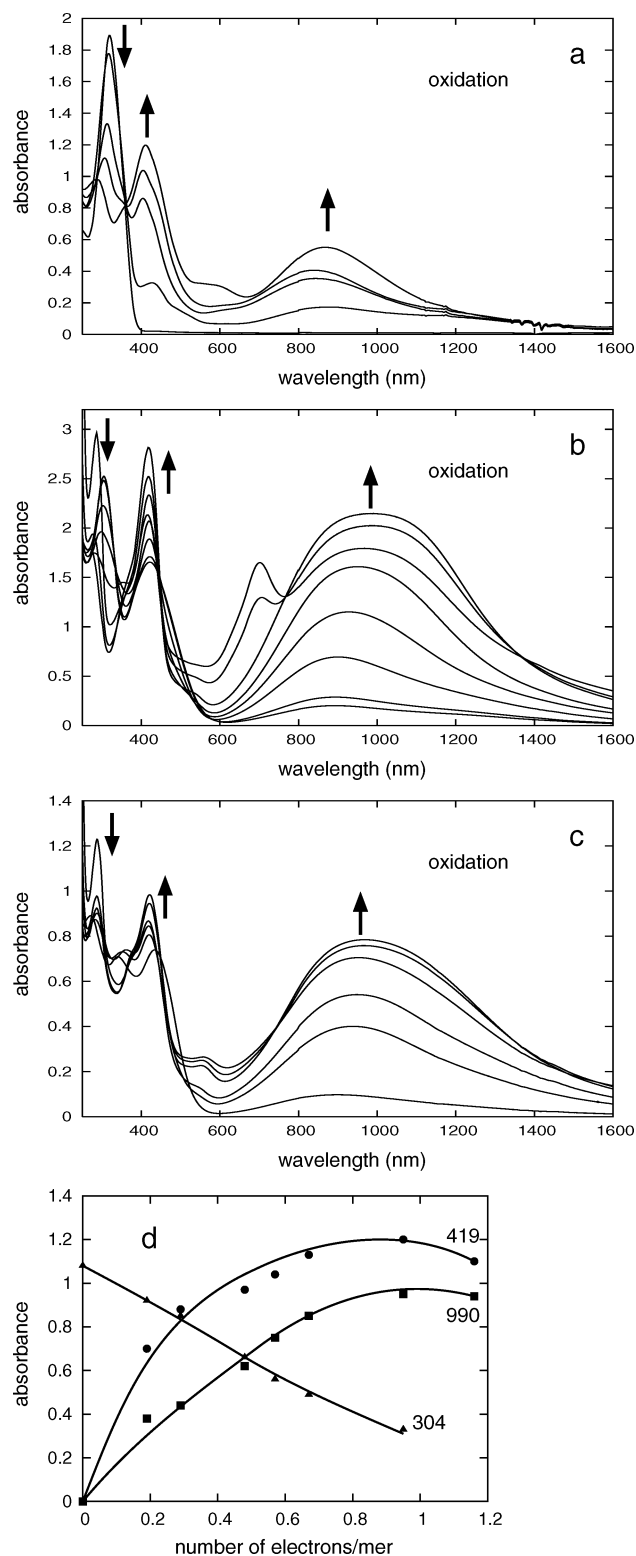


Figure 2. UV-vis-NIR spectra of poly(*m-p*-anilines): (a) **PA1** oxidized with NO_2BF_4 in CH_2Cl_2 ; (b) **PA1** oxidized with CPB in $\text{CH}_2\text{Cl}_2/\text{TFA}$ (9:1) solution; (c) **PAB1** oxidized with CPB in $\text{CH}_2\text{Cl}_2/\text{TFA}$ (9:1) solution; (d) absorbance of **PA1** oxidized with CPB vs the theoretical number of electrons removed from polymer unit (measured at 304, 419, and 990 nm, the concentration of polymer, $c = 5 \times 10^{-5}$ M).

should be noted here that the indicated oxidation states are formal, i.e., calculated from the oxidant to polymer molar ratio and assuming 100% oxidation yield. It is also assumed that the oxidation results in the formation of radical cations as the sole charge-spin configurations. Taking into account the polymer

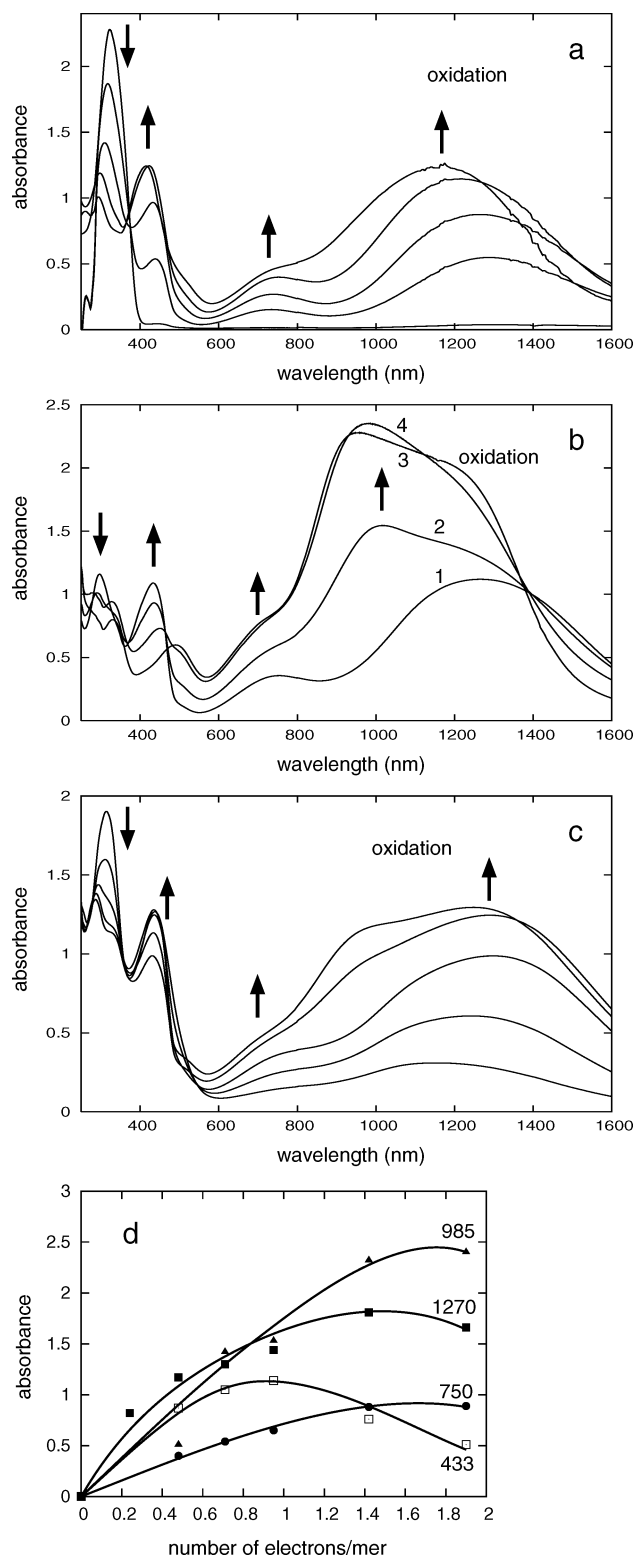


Figure 3. UV-vis-NIR spectra of poly(*m-p-p*-anilines): (a) **PA2** oxidized with NO_2BF_4 in CH_2Cl_2 ; (b) **PA2** oxidized with CPB in $\text{CH}_2\text{Cl}_2/\text{TFA}$ (9:1) solution; (c) **PAB2** oxidized with CPB in $\text{CH}_2\text{Cl}_2/\text{TFA}$ (9:1) solution; (d) absorbance of **PA2** oxidized with CPB vs the theoretical number of electrons removed from polymer unit (measured at 433, 750, 985, and 1270 nm, the concentration of polymer, $c = 5 \times 10^{-5}$ M).

titration experiments monitored by UV-vis-NIR spectroscopy (vide supra), this assumption is justified only for the oxidation states involving, at the most, abstraction of one electron per repeat unit since further oxidation leads to the appearance of the absorption band characteristic of spinless dications formed

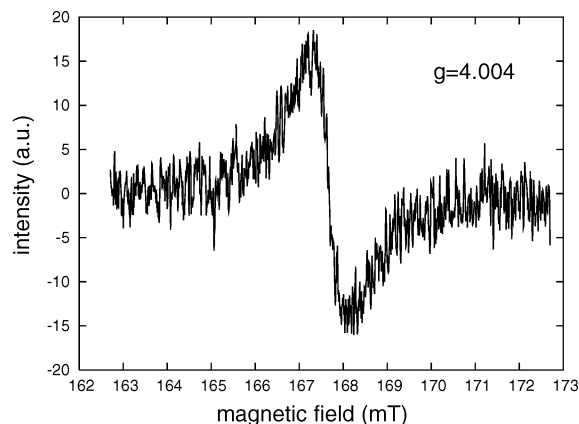
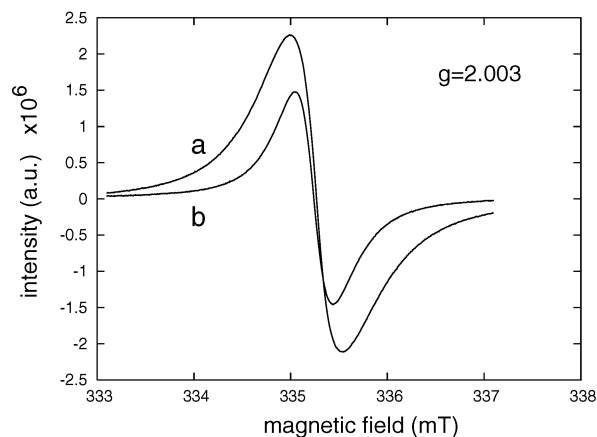


Figure 4. EPR spectrum of **PA1** oxidized to radical cations in $\text{CH}_2\text{Cl}_2/\text{TFA}$ (9:1) solution—frozen solution recorded for the $\Delta M_s = \pm 1$ (left) and for the $\Delta M_s = \pm 2$ (right) at (a) 6 K and (b) 13 K.

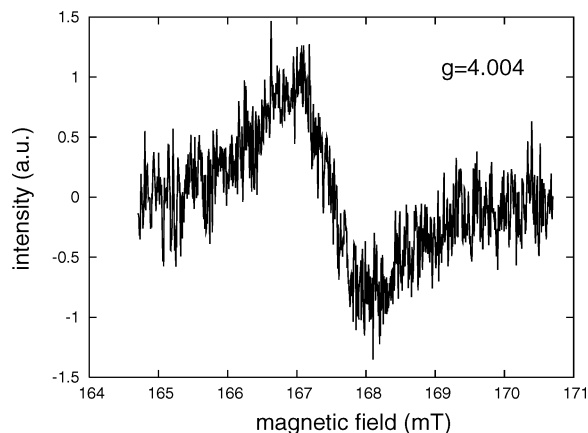
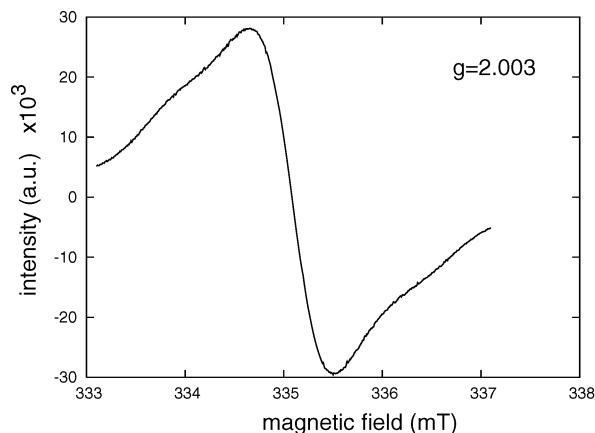


Figure 5. EPR spectrum of **PA2** oxidized to radical cations in $\text{CH}_2\text{Cl}_2/\text{TFA}$ (9:1) solution—frozen solution recorded for the $\Delta M_s = \pm 1$ (left) and for the $\Delta M_s = \pm 2$ (right) at 6 K.

through radicals recombination. We were tempted to confirm this by quantitative EPR studies. The number of spins can be calculated through double integration of the EPR signals; however, the results may bear significant errors mainly related to the determination of the polymer concentration and the quantity of the polymer solution in the EPR tube. Despite these limitations which lead to the determination error of ca. 30%, the obtained results indicate that the abstraction of one electron per repeat units results in the formation of stable radical cations which do not recombine. **PA1**¹⁺ and **PA2**²⁺ show 0.9 and 0.7 spin per repeat unit, respectively, proving that radical cations are the dominant charge-spin configurations in this oxidation state of the polymers. For higher oxidation states spin recombination may take place which cause that the measured spin concentration is lower than that predicted for the formation of radical cations as the sole charge-spin configurations. For example, **PA2**²⁺ shows only 0.6 spin/repeat unit which is less than half of the predicted value. This means that 50% of the created spins were removed via their recombination to spinless dications. These findings are consistent with the results of the UV–vis–NIR studies (vide supra).

The ESR spectrum of **PA1**¹⁺ at 6 K shows one line with the width of 0.6 mT in the $\Delta M_s = \pm 1$ region and a second line at half field for the $\Delta M_s = \pm 2$ transition (Figure 4). This indicates the presence of high-spin species in the oxidized polymer solution. The intensities of both lines decrease with increasing temperature similarly as observed by Janssen et al.¹ for oligoanilines and by us for poly(*m-p*-anilines).¹⁵ The ESR spectrum of **PAB1**³⁺ recorded under the same conditions is broader (0.8 mT) than that of **PA1**¹⁺ for the $\Delta M_s = \pm 1$ transition

and has comparable width to that of **PA1**¹⁺ in the $\Delta M_s = \pm 2$ region. The broadening of the signal can be ascribed to the increase of dipolar spin–spin coupling in the quasi-three-dimensional branched polymer (**PAB1**) in comparison to the linear one (**PA1**). In the case of **PA2**, which contains *m-p-p*-units, one can consider a ferromagnetic coupling of spins linked to *m*-phenylene ring and an antiferromagnetic interaction of spins linked to *p*-phenylene. When **PA2** was oxidized to the **PA2**¹⁺ state (one radical cation in the unit), only one unresolved line at $g = 2.003$ was observed and the resonance at half field was not recorded. However, the ESR spectrum of **PA2**²⁺, which formally corresponds to the presence of two radical cations in the polymer unit, shows a broad line of 0.8 mT for the $\Delta M_s = \pm 1$ transition, as well as a line for the $\Delta M_s = \pm 2$ region (Figure 5).

Moreover, the signal with $g = 2.003$ shows some deformations, suggesting an increase of the multiplicity of the system. Thus, we can conclude that, even for the **PA2**²⁺ oxidation state, in the polymer containing *m-p-p*-units, ferromagnetic interactions dominate and the polymer shows the high-spin behavior.

The ESR spectrum of **PAB2**²⁺ shows also two signals for the $\Delta M_s = \pm 1$ and $\Delta M_s = \pm 2$. Surprisingly, the signal for $g = 2.002$ is narrower than that of **PA2**²⁺.

Summarizing, in the spectra of all oxidized polymers we have observed the lines at half field characteristic of the high-spin state. The lack of the fine structure in the $\Delta M_s = \pm 1$ region does not allow us to estimate the zero field splitting parameters. Moreover, to determine the definite spin multiplicity of the polymers oxidized to radical cations, it is necessary to carry

out the electron spin transient nutation measurements. This type of study will be performed in the near future.

Conclusions

To summarize, we have shown that alternating poly(*m-p*-anilines) and poly(*m-p-p*-anilines) can be oxidized to radical cations via electrochemical or chemical methods. The presence of radical cations was proven by the appearance of new bands in the UV-vis-NIR spectra. The shape of these new bands depends on the oxidation media. The oxidation in acidic medium leads to the formation of localized radical cations which is related to the protonation of amine groups of polymers. Radical cations form high-spin state confirmed by EPR measurements. In the case of poly(*m-p-p*-anilines) a ferromagnetic interaction caused by *m*-coupling dominates over an antiferromagnetic one realized by *p*-coupling.

Acknowledgment. We wish to acknowledge financial support from the Committee of Scientific Research in Poland (KBN, Grant No. 3 T09A 100 29).

References and Notes

- (1) Wienk, M. M.; Janssen, R. A. J. *J. Am. Chem. Soc.* **1997**, *119*, 4492–4501.
- (2) Wienk, M. M.; Janssen, R. A. J. *J. Am. Chem. Soc.* **1996**, *118*, 10626–10628.
- (3) Hartwig, J. F. *Acc. Chem. Res.* **1998**, *31*, 852–860.
- (4) Wolfe, J. P.; Wagaw, S.; Marcoux, J. F.; Buchwald, S. L. *Acc. Chem. Res.* **1998**, *31*, 805–818.
- (5) Ito, A.; Taniguchi, A.; Yamabe, T.; Tanaka, K. *Org. Lett.* **1999**, *1*, 741–743.
- (6) Selby, T. D.; Blackstok, S. C. *J. Am. Chem. Soc.* **1999**, *121*, 7152–7153.
- (7) Ito, A.; Ono, Y.; Tanaka, K. *Angew. Chem., Int. Ed.* **2000**, *39*, 1072–1075.
- (8) Ito, A.; Ino, H.; Matsui, Y.; Hirao, Y.; Tanaka, K.; Kanemoto, K.; Kato, T. *J. Phys. Chem. A* **2004**, *108*, 5715–5720.
- (9) Hirao, Y.; Ino, H.; Ito, A.; Tanaka, K.; Kato, T. *J. Phys. Chem. A* **2006**, *110*, 4866–4872.
- (10) Michinobu, T.; Takahashi, M.; Tsuchida, E.; Nishide, H. *Chem. Mater.* **1999**, *11*, 1969–1971.
- (11) van Meurs, P.; Janssen, R. A. J. *J. Org. Chem.* **2000**, *65*, 5712–5719.
- (12) Goodson, F. E.; Hauck, S. I.; Hartwig, J. F. *J. Am. Chem. Soc.* **1999**, *121*, 7527–7539.
- (13) Michinobu, T.; Inui, J.; Nishide, H. *Org. Lett.* **2003**, *5*, 2165–2168.
- (14) Fukuzaki, E.; Nishide, H. *J. Am. Chem. Soc.* **2006**, *128*, 996–1001.
- (15) Kulszewicz-Bajer, I.; Zagórska, M.; Wielgus, I.; Pawłowski, M.; Gosk, J.; Twardowski, A. *J. Phys. Chem. B* **2007**, *111*, 34–40.
- (16) Genoud, F.; Guglielmi, M.; Nechtschein, M.; Genies, E.; Salmon, M. *Phys. Rev. Lett.* **1985**, *55*, 118–121.

MA070111J